INVESTIGATIONS OF POLYCRYSTALLINE SILICON LAYERS DEPOSITED BY HOT WIRE CVD

A. Breymesser, V. Plunger, M. Ramadori, V. Schlosser
Institut für Materialphysik der Universität Wien
A-1090 Wien, Strudlhofgasse 4, Austria, phone (++43 1) 586 3409, e-mail: Viktor.Schlosser@Univie.ac.at
M. Nelhiebel, P. Schattschneider
Institut für Angewandte und Technische Physik, Technische Universität Wien
A-1040 Wien, Wiedner Hauptstraße 8-10, Austria
D.Peiro, C. Voz, J. Bertomeu, J. Andreu
Departament de Fisica Aplicada i Electrònica, Universitat de Bercelona
E-08028 Barcelona, Av. Diagonal 647, Spain

ABSTRACT: We report about some physical properties of undoped polycrystalline silicon layers deposited at substrate temperatures betweenn 190°C and 275°C by hot-wire CVD on glass substrates. The crystallinity was proofed by Raman- and ultraviolet reflectance spectroscopy. The observed optical band gap was found to be very close to that one of monocrystalline silicon. A dependence of (i) the cluster size of the crystallites (ii) the density of defect states within the bandgap and (iii) the lifetime mobility product, $\mu\tau$, on the substrate temperature was found. The highest observed value for $\mu\tau$ was $9.4\times10^{-7} cm^2V^{-1}$.
Keywords: Silicon - 1: Polycrystalline - 2: Photoelectric Properties - 3

1. INTRODUCTION

In the past few years thin crystalline silicon films have attracted great attention for thin film photovoltaic applications [1]. Polycrystalline films have the potential to combine the advantage of a low temperature deposition technique similar to the deposition of amorphous silicon with the high long term stability known from crystalline silicon solar cells. Various physical and chemical vapour deposition techniques have been introduced for the preparation of crystalline silicon on glass [2,3,4,5,6]. Since the substrates is preferentially borosilicate floatglass the substrate temperature is limited to about 500°C. In order to achieve high deposition rates and stimulate crystallite formation the deposition technique is usually accompanied by introducing additional energy for e.g. by means of a microwave plasma to the deposition system. Sometimes a posttreatment of the deposited layers by a prolonged solid phase crystallization or by rapid thermal annealing procedures are applied [7,8]. In this paper we report about investigations of undoped polycrystalline silicon layers grown on glass and silicon substrates by the hot-wire CVD process (HWCVD) which is sometimes referred to as catalytic CVD [5]. The process allows reasonable deposition rates and doping control. Crystalline layer growth has been observed at substrate temperatures as low as 190°C. In this work we report of some of the optical (section 3.1) and electrical (section 3.2) properties of undoped polycrystalline silicon layers made by HWCVD.

2. EXPERIMENTAL

The polycrystalline silicon films were deposited onto Corning 7059 glass and Si (111) substrates in a new HWCVD multichamber reactor equipped with a load-lock chamber and base pressures lower than 10^{-8} *mbar*. Details on the experimental set-up are described elsewhere [9]. A gas mixture consisting of 2*sccm* and 18*sccm* of silane and hydrogen respectively, was introduced into the deposition chamber with inverted geometry, designed so as to minimize the formation of pinholes due to eventual powder formation. The dissociation of the gases was obtained by means of a hot tungsten wire with a diameter of 1.0*mm* at temperatures in the range between 1610°C and 1650°C, placed under the substrates at a fixed distance of 6*cm*. A set of samples (Table I) was obtained by varying the substrate temperature (T_s) between 190°C and 250°C at a process pressure of 1.1×10^{-2} *mbar*. Another sample (230198) was obtained by using the same technological parameters at a process pressure of 4.5×10^{-3} *mbar*.

Table I: Deposition conditions of the polysilicon layers.

Sample	Filament temperature [°C]	Substrate temperature [°C]	Process pressure [mbar]
190198	1610	190	1.2×10^{-2}
190198B	1610	225	1.3×10^{-2}
200198	1610	250	1.1×10^{-2}
200198B	1610	275	1.3×10^{-2}
230198	1650	190	4.5×10^{-3}

The thickness of the deposited layers was typically about $1\mu m$. The layers have been investigated by Raman spectroscopy and ultraviolett reflectance spectroscopy in order to proof their crystallinity. The observed Raman spectra for all samples clearly show an intense line close to $519cm^{-1}$. For monocrystalline silicon the Raman-active $\Gamma_{25'}$ mode is leading to a sharp peak at $519.5cm^{-1}$ [11]. For two samples the spectra are shown in figure 1. A slight shift towards smaller wavenumbers and some broadening of the linewidth can be seen. However a shoulder at lower wavenumbers which is due to a peak around $480cm^{-1}$ arising from an amorphous phase was not resolved [6].

The ultraviolett reflectance spectra were taken with a Perkin Elmer 552 spectrometer. The bandwidth of the incident light was set to $1nm$. The sample compartment was merged with nitrogen during the measurements.

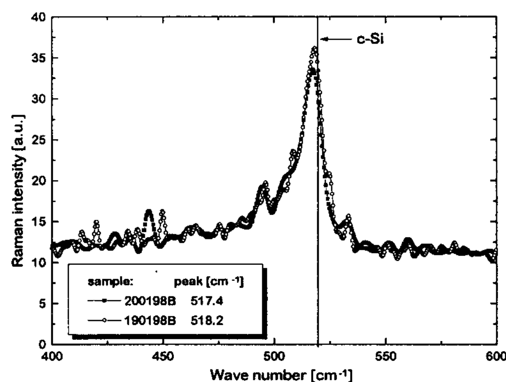

Figure 1: Raman spectra of two samples of undoped polycrystalline silicon films on glass substrates. The line at 519.5 cm^{-1} indicates the $\Gamma_{25'}$ mode in monocrystalline silicon.

The measured reflectance data in the photon energy range between $3eV$ and $6eV$ were numerically differentiated and normalized to the absolute reflectance in order to determine the position of the maxima. For monocrystalline silicon a maximum at $4.56eV$ - attributed to the E_2 interband transition [12] - and $3.41eV$ - attributed to the E_1 transition [12] - and a minimum at around $5.25eV$ is expected. For amorphous silicon a maximum around $4.0eV$ is typical [13]. A mixed state of amorphous and crystalline phases usually is leading to a superposition of the peak at $4.56eV$ caused by the crystalline phase and the "amorphous" peak at $4.0eV$ which sometimes leads to the assumption that the crystalline E_2 transition is shifted towards lower photon energies.

In spite of the surface roughness of the layers which can be estimated from figure 2 which altered the spectra somewhat we found the E_1 and E_2 transition nearly unchanged from the values for monocrystalline silicon and there was no evidence for an amorphous phase.

The surface topography of the samples was inspected by means of a scanning atomic force microscope (AFM) which was run in the contact mode in ambient air. The surface topography of an $2\times2\mu m^2$ area of four samples is shown in figure 2. The depth scale for all pictures is around $50nm$. A rather rough surface topography consisting of grains and spaces was observed. Earlier investigations of HWCVD samples by transmission electron microscopy (TEM) and AFM were leading us to the conclusion that the grains seen in the AFM pictures are not single crystals. Correlating the sizes of the grains with the substrate temperature it seems that with increasing substrate temperature the grains are clustering together.

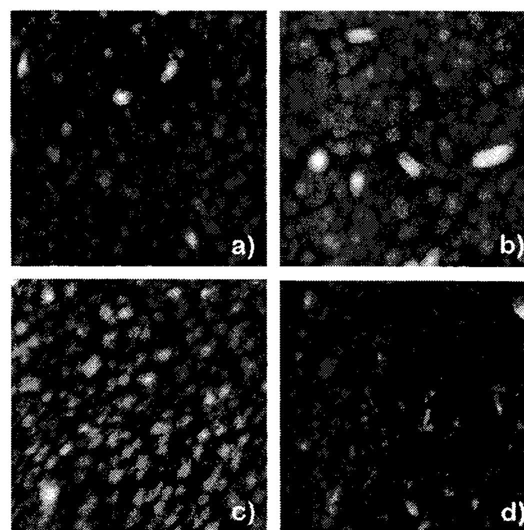

Figure 2: Surface topography of an area of $2\times2\mu m^2$ of the polycrystalline silicon layers obtained by scanning atomic force microscopy. The depth scale is about $50nm$. Samples 190198 a), 190198B b), 200198 c) and 200198B d).

3. RESULTS

3.1 Optical properties

Optical absorption spectra were obtained by the photothermal deflection spectrometry technique (PDS) with a transversal geometry. Comparing the sample's signal with the one obtained with a thick graphite sample, which is optically dense in the whole spectrum, an absolute value of the absorption of the sample is deduced. The result for sample 190198 is shown in figure 3 together with the result of a calculation of the absorption coefficient based on the measured transmittance and reflectance of the sample. Similar results were obtained on the other samples except for sample 230198. For comparison purposes the absorption coefficient of monocrystalline silicon is shown. The absorption observed for photon energies below $1.12eV$ is attributed to band tails caused by defect related levels within the bandgap. Compared to earlier results on HWCVD samples

the sub bandgap absorption was significantly lowered indicating a lower defect density.

The reflectance and transmittance of the undoped polysilicon samples were measured in the wavelength range from 190*nm* to 2600*nm* with a resolution of 1*nm*. The optical thickness of the layers as well as the index of refraction and the extinction coefficient was evaluated with the help of the computer program "FilmWizard". The evaluation was done by completely suppressing the sub bandgap contributions to the absorption in order to define a optical bandgap ε_{opt}, of the polycrystalline films. The result of the calculated absorption can be seen in figure 3. The inset shows how the optical gap was determined. Following the well known procedure for single crystal silicon assuming an indirect bandgap transition a plot of the square root of the product of the absorption coefficient and the photon energy can be approximated by two straight lines. The extrapolation results in two photon energies ε_1 and ε_2 according to equation 1.

$$\begin{aligned} \varepsilon_1 &= \varepsilon_{opt} - \hbar\omega_{ph} \\ \varepsilon_2 &= \varepsilon_{opt} + \hbar\omega_{ph} \end{aligned} \qquad (1)$$

$\hbar\omega_{ph}$ is the energy contribution of the phonon involved in the bangap transition. Except for sample 230198 - for which ε_{opt} was calculated to be about 1.6*eV* - the determined values for ε_{opt} are close to the value for crystalline silicon (see table II). Although the physical interpretation of ε_{opt} requires a better knowledge about the band structure in polycrystalline silicon it permits a fast comparison of the optical absorption near the band gap of different polysilicon samples.

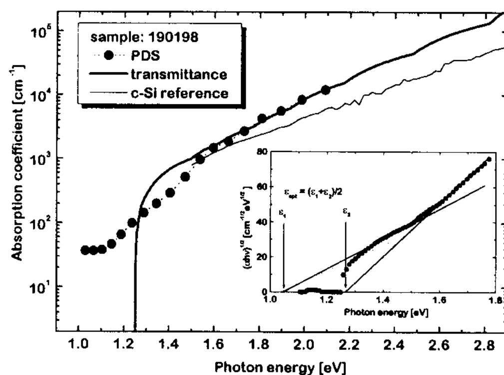

Figure 3: Absorption coefficient for the sample 190198 as determined by PDS and computed values derived from the transmittance spectra not taking into account the band edges. These data were taken to define the optical gap as shown in the inset.

3.2 Electrical properties

For electrical measurements chromium contacts were evaporated onto the samples surfaces. Two type of structures were prepared: (i) four perpendicular to the sample length applied stripes in a line and (ii) four point contacts at the edges of a quadratic sample according to the Van der Pauw geometry. The electrical measurements were made by the use of a current source (Keithley type 224) and an electrometer (impedance greater than $10^{14}\Omega$, Keithley 616). The line arrangement - sample width about 0.5*cm*, spacing between the two inner contacts about 0.9*mm* - was used to determine the temperature dependence of the conductivity. The measurements were done in a temperature controlled compartment in the dark in ambient atmosphere. In figure 4 the Arrhenius plots of three samples are shown. Around room temperature the activation energy E_{act}, is given by a deep level defect. Increasing the temperature a saturation region can be observed followed by an interband activation towards higher temperatures. The determined activation energy is taken as the conductivity gap ε_{cond}. At even higher temperatures a third activation takes place with energies >1.6*eV*. This activation can only be seen when the samples were heated in air. In vacuum the intrinsic activation remains constant towards the highest measured temperatures which indicates that in air a structural change probably caused by the presence of oxygen takes place. In previous investigations with electron energy loss spectroscopy (EELS) of a cross section of HWCVD silicon layers it was observed that oxygen is inhomogeneously incorporated in the layers. The influence of oxygen on the electrical properties is currently under investigation by means of EELS and atomic mass spectroscopy.

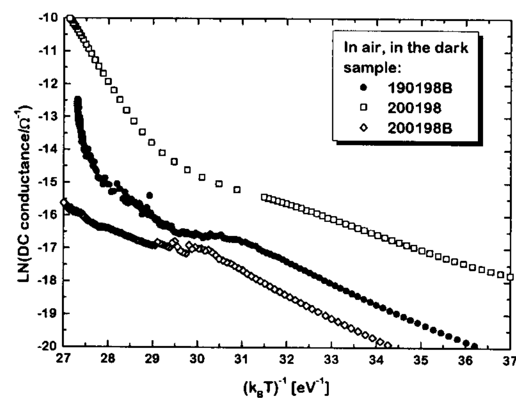

Figure 4: Arrhenius plot of the sample conductance. Three regions can be distinguished: At low temperatures an extrinsic behaviour with activation energies ~ 0.5*eV* which saturates. At increasing temperatures the intrinsic range with activation energies ~1*eV* and at high temperatures activation energies >1.6*eV* are observed.

Samples in Van der Pauw geometry were used for magneto transport measurements. The measurements were carried out in air at temperatures where the activation of the deep level defect saturates (temperature about 360*K*). The evaluation of the car-

rier concentration from Hall measurements was done by the relation given in equation 2.

$$R_H = \frac{r_H}{qn} \tag{2}$$

R_H is the Hall coefficient, r_H is the scattering factor assumed to be 1, q is the elementary charge and n is the majority carrier concentration. The sign of R_H determines whether electrons or holes are the majority carriers. This preliminary data evaluation leads to typical carrier concentrations in the range of $10^{14}cm^{-3}$. Negative as well as positive values of R_H have been observed. In order to take into account the contribution of both types of carriers to the conductivity a more detailed analysis of the ambipolar Hall effect will be necessary.

Steady State Photoconductivity (SSPC) measurements were carried out to obtain the mobility-lifetime product ($\mu\tau_{ph}$). Monochromatic light of $620nm$ ($\sim 2eV$) was used to illuminate the sample, producing band to band transitions. The monochromatic light was obtained from a halogen lamp and an interference filter (FWHM about $10nm$). A change of around two orders of magnitude in the carrier generation was obtained by increasing the illumination level by means of the variation of the voltage supply of the lamp. A calibrated detector was used to obtain the irradiance in photons/cm^2. This value is translated to carrier generation using the absorption coefficient and thickness of the sample. The $\mu\tau_{ph}$ product was obtained from the log-log plot of the conductivity, σ_{ph}, versus the generation rate, G, where $\sigma_{ph}=q\mu\tau_{ph}G$ [10].

All the experimental results are summarized in table II.

Table II: Optical and electrical properties of the undoped polycrystalline silicon films.

Sample	ε_{opt} [1] [eV]	ε_{cond} [eV]	E_{act} [2] [eV]	n [3] $\times 10^{13}$ [cm^{-3}]	$\mu\tau \times 10^{-8}$ [cm^2/V]
190198	1.17	1.02	.605	-17	2.3
190198B	1.19	.96	.603	+6	2.6
200198	1.28	~.9	.462	-7	1.9
200198B	1.14	-	.676	-	.44
230198	~1.5	-	.217	-	94

1) determined from transmittance and reflectance calculations.
2) Activation energy around room temperature.
3) Carrier concentration determined from Hall measurements at $360K$. A negative sign indicates an electron concentration, a positive sign a hole concentration.

4. CONCLUSIONS

The set of 4 samples deposited at almost identical process conditions except for the substrate temperature, T_S, exhibits a clear dependence of the physical parameter on the substrate temperature. The mean cluster size of the crystalline grains increases with increasing T_S. The sub bandgap absorption was found to increase with increasing T_S which can be attributed to an increase of the density of deep defect levels within the bandgap. The origin of these defect levels is believed to be mainly caused by dangling bonds which are not passivated by hydrogen atoms [10]. The increase of defect levels with T_S causes the shrinkage of the conductivity gap whereas the optical gap remains unchanged. Up to a substrate temperature of $250°C$ the the $\mu\tau_{ph}$ product is not significantly changed and is about $2\times10^{-8}cm^2V^{-1}$. Above 250°C it decreases dramatically down to $0.44\times10^{-8}cm^2V^{-1}$.

ACKNOWLEDGEMENT

We thank Dr. H. Kuzmany that we could use his scanning atomic force microscope.

REFERENCES

[1] S. K. Deb, Curr. Opin. Solid State Mat. Sci. **3** (1998) 51.

[2] M. Tzolov, F. Finger, R. Carius P. Hapke, J. Appl. Phys. **81** (1997) 7376.

[3] B. Sanghoon, A. K. Kalkan, C. Shangcong, S. J. Fonash, J. Vac. Sci. Technol. **A16** (1998) 1912.

[4] J. Guillet, A. R. Middya, J. Hue, J. Perrin, B. Equer, J. E. Bourrée, Proc. 14th EC PVSEC, H.S. Stephens & Ass. Bedford, UK 1997, 1475.

[5] R. Iiduka, A. Heya, H. Matsumura, Solar Energy Mater. Solar Cells, **48** (1997) 279.

[6] P. Müller, W. H. Holber, R. Gat, W. Henrion, E. Neubauer, V. Schlosser, L. Sieber, W. Fuhs, this conference.

[7] R. Rüther, J. Livigstone, N. Dytlewski, Thin Solid Films **310** (1997) 67.

[8] T. Mohammed-Brahim, M. Sarret, D. Briand, K. Kis-Sion, L. Haji, O. Bonnaud, Philosophical Magazine B, **76** (1997) 193.

[9] D. Peiró, J. Bertomeu, C. Voz, J. Andreu. *To be published.*

[10] M. Goerlitzer, N. Beck, P. Torres, J. Meier, N.Wyrsch, A.Shah. J. Appl. Phys. **80** (1996) 5111.

[11] S. Veprec, F. A. Sarott, Z. Isobal, Phys. Rev. **36** (1987) 3344.

[12] Landolt Börnstein, New Series Group III, **17**, subvol. a, O. Madelung Ed. (Springer 1982).

[13] F. Kuchar, V. Schlosser, *private communication.*